International Journal of Advanced Technology in Engineering and Science
Vol. No. 11, Issue No. 06, June 2023
www.ijates.com
ijates
ISSN 2348 - 7550

A Comparison of Cosmic-Ray Modulation During the Passage of CIRs and ICMEs

Udayveer Vikram Singh Bundela
Research Scholar, Research Center- Govt.PG(Auto.) Satna (M.P.)
Email - udayraja495@gmail.com
Dr Sushil Kumar Sharma
Guide, Govt. PG College, Satna (M.P.)
Email - bcs.sks@gmail.com
C.M.Tiwari
Department of Physics, APS University, Rewa (M.P.)
Email- cmtiwari_2005@yahoo.com

Abstract:
We contrast the grandiose beam reaction with interplanetary coronal mass Ejection (ICMEs) and corotating cooperation districts (CIRs) during their entry in close Earth space. We concentrate on the general significance of different designs/highlights recognized during the entry o1 the ICMEs and CIRs saw during Cycle 23 (1995 — 2009). The recognized ICME structures are the shock front, the sheath, and the CME ejecta. We confine the shock appearance time, the section o1 the sheath locale, the appearance of ejecta, and the end season of their entry. Likewise, we disconnect the CIR appearance, the related forward shock, the stream interface, and the converse shock during the section of a CIR. For the inestimable beam power, we use the information from high counting rate neutron screens. Notwithstanding neutron screen information, we use close synchronous and same time-goal information of interplanetary plasma and field, in particular the sunlight based breeze speed, the interplanetary attractive field (IMF) vector, and its vari-ance. Further, we likewise use a few inferred interplanetary boundaries. We apply the technique for the superposed-age examination. As the plasma and field properties are different during the section of various designs, both in ICMEs and CIRs, we deliberately fluctuate the age time in our superposed-age examination individually. Along these lines, we concentrate on the job and ef-fects of every one of the distinguished individual designs/highlights during the section of the ICMEs and CIRs. Relating the properties of different designs and the comparing varieties in plasma and field boundaries with changes of the enormous beam power, we distinguish the rela-tive significance of the plasma/field boundaries in impacting the plentifulness and time profiles of the astronomical beam force varieties during the entry of the ICMEs and CIRs.

Keywords: CR rays ‘Solar modulation CME,CIRF Forbush

1. Introduction

Interplanetary partners of coronal mass discharges (ICMEs) and corrugating communication districts (CIRs) are two significant enormous scope structures in the interplanetary space. Dur-ing the section of these designs, decline in the cosmic astronomical beam (GCR) power has been noticed both by space-borne and ground-based vast beam instruments with fluctuate ing amplitudes and time profiles The ICMEs going through close Earth space might be related with advanced shock and sheath locales toward

the front or they might be just a transition rope structure moving with speed not the same as the shock-related ICMEs. Many examinations have been done to comprehend and demonstrate the astronomical beam diminishes during the entry of the ICMEs CIRs are shaped because of the cooperation of a high velocity stream with the more slow ambi-ent sunlight based breeze. These designs proliferating with rapid in space might possibly have a forward shock related with them. The infinite beam discouragements during the pas-sage of rapid streams/CIRs also have been concentrated tentatively and displayed by analysts over the numerous years).The vast majority of the previous examinations have been bound to the investigation of the nature and wellsprings of transient/Forbush diminishes because of the ICMEs and corotating despondency in grandiose beam in-strained quality because of CIRs and high velocity sunlight based breeze streams. There have been put forth many attempts to figure out the job of individual designs inside ICMEs and CIRs, in any case, one actually needs comprehension of the fundamental actual cycles. Since the plasma/tield properties at the appearance and during the section of these unmistakable designs in ICMEs and CIRs probably won't be comparable, it will be fascinating to concentrate on the job of these particular designs in ICMEs and CIRs in affecting the GCR force.The in situ plasma and field perceptions from the High level Piece Traveler (Pro) and Wind shuttle have been broadly used to recognize close Earth ICMEs and CIRs for a persistent period spreading over the entire of Sun powered Cycle 23 (Richardson and Stick, 2010; Jian, Russell, and Luhmann, 2011). An overview of ICMEs and CIRs gives se-lection rules and the timings of different particular highlights and designs saw during their entry (Jan et a/. 2006a, 2006b).The point of this study is two-overlay. To start with, to analyze the GCR viability of the ICMEs and CIRs identified during 1995 — 200 Second, we concentrate on the overall significance of different dis-coloration highlights/structures in ICMEs and in CIRs in impacting the size and time favorable to document of coming about diminishes in astronomical beam force. The unmistakable highlights/structures distinguished in shock-related ICMEs concern the shock/irregularity followed by the sheath district shaped because of pressure of the encompassing plasma and field by the attractive deterrent, for example essentially the CME ejecta, which may or probably won't show the transition rope attributes de-forthcoming on the space apparatus direction through the ICME In the event of CIRs, the beginning time, the hour of stream interface (framed because of pressure of slowwind by rapid sun based breeze) as well as end of CIR have been recognized. The data is likewise accessible regardless of whether a CIR is related with a forward shock. Essentially, it is known regardless of whether a CIR is related with an opposite shock. Brokenness time, overall co-incides with the forward shock time assuming that such shock is related with the CIR. Be that as it may, in the interplanetary information, at times stream connection point is additionally viewed as brokenness (see Jian ct al., 2006a, 2006b). We concentrate because of the CIR overall on its appearance, forward shock (when related), stream interface and the end (entry) ot CIR on the abundancy and time profile of GCR-power gloom. Likewise, we additionally look for the interplan-etary plasma field parameter(s) that play(s) significant job in impacting the adequacy and the time profile of GCR-power variety during the entry of the ICMEs and CIRs.

2. Data and Method

We have applied the technique for the superposed-age examination on enormous beam as well as in-terplanetary plasma and field information using the beginning season of various ICME/CIR structures as ages in our examination. The superposed-age technique is a factual examination procedure which is much of the time used to devil strate an impact or a periodicity. With the assistance of this technique, we concentrate on the impacts of different sunlight based/interplanetary peculiarities on astronomical beam power. We, first of all, chose the occasions with specific standards. Having characterized the measures of an occasion, the information of an explicitly planned stretch (72 hours prior and 360 hours after the beginning of an occasion) were removed from the full information base. Then the hourly arrived at the midpoint of information of the chose time stretch were superposed on one another taking the no time as the beginning season of occasions. The outcomes so got are supposed to uncover the unique part

of the reaction. By efficiently changing the ages, individually, and examining the hourly information of the GCR power and close synchronous sun based breeze plasma/field information, we have attempted to concentrate on their job in influence ing the GCR force on their appearance and during the entry of various districts of particular plasma/field properties. For ICME and CIR information, the arranged indexes of ICMEs and CIRs were used (http://www- ssc.igpp.ucla.edu/jlan/Expert/Level3/). The beginning/end season of different designs/highlights in ICMEs, like the beginning of an ICME, the attractive obsta-cle, and the end season of the ICME as well as the hour of the irregularity is given in the ICME index. In the stream cooperation district (SIR) list, begin and end seasons of a CIR as well as irregularity and stream interface timings are given (see Jian et al., 2006a, 2006b for subtleties). We examined 291 occasions of the ICMEs, out of which 181 are related with a shock. Out of complete 416 CIRs occasions, 76 are related with a forward shock. For the grandiose beam power, we have utilized the neutron screen information of two areas on the Earth: Oulu (scope = 64.05 N, longitude = 25.47 E, cut-off inflexibility fi, = 0.81 GV) and Newark (scope = 39.7 N, longitude = 75.7 W, cut-off unbending nature fi, = 2.09 GV). Information for two neutron-screen stations were used to guarantee that the noticed varieties in the GCR power are not because of any neighborhood impacts however are genuine, with practically comparable transient profiles that vary in adequacy because of the different cut-off rigidities of the two areas. The OMNI Electronic information (omniweb.gsfc.nasa.gov) of the plasma/field boundaries, in particular, the sun based breeze speed [V: km s 1], the IMF vector [F: nT], the standard deviation of the IMF vector nT], the items IV [mV m°'], which has the component of electric field, and FV' [inV s°'], which has the component of the time variety of the electric potential, have been Used in this examination.

Table 1 Middling GCR amount decrease [AI: la] at Oulu and Newark neutron monitors, peak principles of plasma and charismatic field parameters [Yp , Fpp F)max• ( ) max• and (FY2)] and boosts in these bounds [A V, A F, F A(FV), and A(FV2)] due to the ICMEs and CIRs detected during 1995 —2009. Zero hour corresponds to start time of the specific event.

Interplanetary structure/group	No.	A/ (Oulu)	*II* (Newark)	[km s*^{1}]	AV [km s*^{1}]	*Fpp* [nT]	*AF* [nT]	(J) [nT]	*F* [nT]	*(FV)* [mV m*^{1}]	*A(FV)* [mV m*^{1}]	*(F* 2) [mV s*^{1}]	*A(F* $^{2)}$ [mV s*^{1}]
ICMEs	291	1.49	.37	514	79	10.42	4.94	5.09	.09	5.90	3.36	3.54	2.38
CIRs	416	0.48	.45	520	168	7.61	3.67	3.54	.18	3.61	2.02	1.80	1.21
ICME with shock	181	2.07	1.90	542	110	11.31	6.10	6.36	4.52	6.87	4.40	4.24	3.13
ICME without shock	110	0.91	0.80	470	34	9.19	3.74	3.90	1.89	4.31	1.68	2.39	1.19
Shock-associated ICMEs with start time and MO time same	22	1.80	2.18	509	62	12.78	8.39	4.62	.96	6.98	4.25	3.88	2.70
Shock-associated ICMEs with start time and MO time different	87	2.32	.82	551	124	12.51	7.60	6.80	.07	7.90	5.58	5.14	4.10
CIR with forward shock	76	0.99	0.89	527	188	8.56	4.85	4.23	3.00	4.15	2.77	1.98	1.47
CIR without forward shock	296	0.41	0.37	514	158	7.42	3.42	3.43	2.05	3.49	1.84	1.78	1.16

International Journal of Advanced Technology in Engineering and Science
Vol. No. 11, Issue No. 06, June 2023
www.ijates.com
ijates
ISSN 2348 - 7550

Table 2 Values *ot* humble Pearson's association coefficients [fi] along by p-value obtained after linear fit amid temporal variation of decrease in the GCR concentration and related plasma and attractive field parameters [V, F, FFV, and F^2 throughout the main and recovery phases of strength depression due to the ICMEs and CIRs associated with/without shock. Durations of the main phase and recovery phase are also given.

Interplanetary structure/group	Duration of the main phase [hrs]	Duration of recovery phase [hrs]	Value of correlation coefficients [fi] between GCR intensity and various parameters									
			V	p-value (10^{-2})	F	p-value (10^{-2})	σ_F	p-value (10^{-2})	FV	p-value (10^{-2})	FV^2	p-value (10^{-2})
						During main phase						
ICMEs	19	153	−0.59	0.60	−0.75	0.02	0.41	**6.89**	−0.68	0.09	−0.65	0.21
CIRs	51		−0.98	0.01	0.26	**6.15**	0.03	**84.9**	−0.35	1.01	−0.72	0.01
ICME with shock	18	215	−0.64	0.02	−0.68	0.01	0.20	**28.7**	−0.61	0.05	−0.55	0.20
ICME without shock	20	95	−0.66	0.17	−0.71	0.04	0.26	**27.2**	−0.68	0.11	−0.65	0.18
CIR with forward shock	52		−0.97	0.01	0.58	0.01	0.68	0.01	0.12	**39.2**	−0.47	0.04
CIR without shock	56		−0.98	0.01	0.03	**80.9**	−0.27	4.13	−0.51	0.01	−0.78	0.01
						During recovery phase						
ICMEs	19	153	−0.87	0.01	−0.80	0.01	−0.02	**78.1**	−0.83	0.01	−0.82	0.01
CIRs	51		−0.77	0.01	0.39	0.01	−0.25	0.01	−0.24	0.01	−0.61	0.01
ICME with shock	18	215	−0.97	0.01	−0.72	0.01	−0.19	0.58	−0.84	0.01	−0.83	0.01
ICME without shock	20	95	−0.93	0.01	−0.76	0.01	0.29	0.39	−0.78	0.01	−0.73	0.01
CIR with forward shock	52		−0.87	0.01	0.20	1.10	−0.03	**71.0**	−0.39	0.01	−0.66	0.01
CIR without shock	56		−0.82	0.01	0.45	0.10	−0.49	0.01	−0.31	0.44	−0.56	0.01

Note. **The p-value in bold indicates that the fi is not statistically significant for the confidence level of 95 %.**

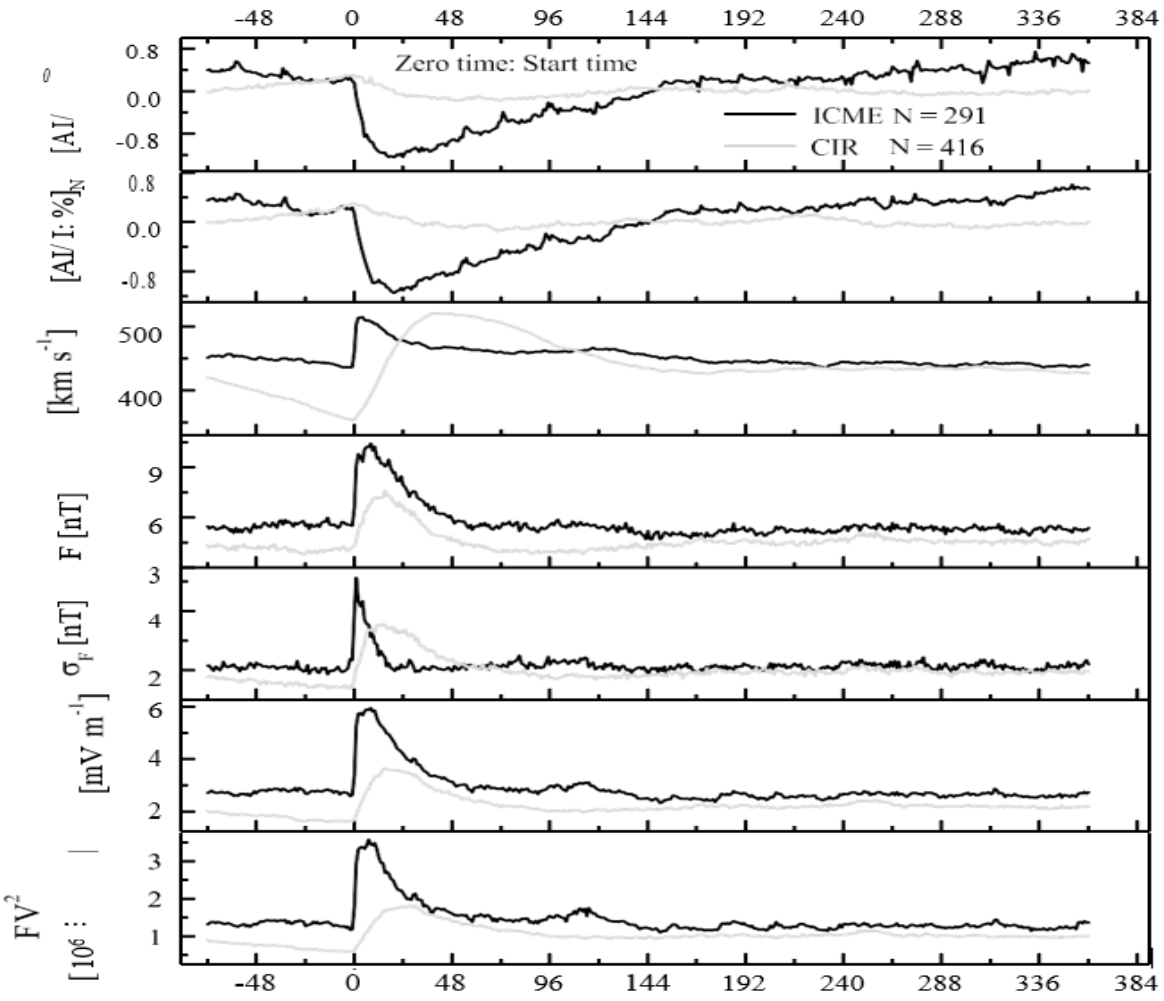

Time [hour]

Figure 1 The superposed-epoch plots of hourly statistics of galactic cosmic ray (GCR) intensity at the Oulu NM *[kI/I:* 9r]$_O$, GCR intensity at the Newark NM *[AI/I:* 9r]$_N$, solar-wind velocity [Y], IMF vector [I], standard deviation in IMF vector [wy], the products *FV* and FV^2 due to ICMEs and CIRs observed during 1995 —2009; zero hour (epoch) corresponds to the arrival time (hour) of the ICMEs and CIRs. N stands for the number of events.

3.1-ICMEs and CIRs: Comparison of Cosmic-Ray and Plasma/Field Variations

Figure 1 shows the superposed-age plots of hourly information of cosmic grandiose beam (GCR) in-strained quality [II/I: %], sun powered breeze speed [Y], interplanetary attractive field (IMF) vector F], standard deviation of IMF vector [• F] , the items [NY], and F Y2. These plots show the varieties of these boundaries 3 days prior and 15 days after the beginning of unsettling influence because of the ICMEs and CIRs saw during 1995 — 2009; party time (age) compares to the appearance time (hour) of the ICMEs and CIRs. For examination, the time variety of various boundaries because of the ICMEs and CIRs are plotted in a similar board on a similar scale. It is seen that there is an enormous contrast in the amplitudes and time profiles of GCR-force discouragements in the two designs; the downturn because of the ICMEs is a lot bigger contrasted with the CIRs. In this way the ICMEs are significantly more GCR powerful than the CIRs (see

Table 1). In the two cases, the GCR gloom begins close to the party time i.c. begin season of the related unsettling influence. The diminishing is quicker because of the ICMEs than the CIRs. Albeit the GCR power recuperated to the pre-decline level following a couple of days on account of the ICMEs, notwithstanding, the downturn perseveres for a more drawn out time frame on account of CIRs. These re- sults affirm past investigations in light of more modest informational collections. Contrasts in the time profiles and amplitudes in vari-ous sun oriented breeze boundaries, alongside GCR power, are self- evident, because of the ICMEs and CIRs. Albeit the improvements in the boundaries [F, oF1 and the items [FV, FV2] are bigger for ICMEs when contrasted with CIRs, the upgrade in the sun based breeze speed [A U] is a lot higher during the entry of CIRs when contrasted with ICMEs (Table 1). How-ever, the change/expansion in the speed on account of the ICMEs is abrupt toward the beginning of the ICME aggravation, while the speed expands gradually to its most extreme on account of CIR-related unsettling influences.
It is notable that the ICMEs and CIRs could conceivably be related with a for-ward shock. The significance of shocks in the transient regulation of cosmic astronomical beams has been featured in many before studies Consequently, we have analyzed the adequacy o1 the ICMEs and CIRs related with shock in de-squeezing the GCR power with the assistance of the superposed-age examination as for the appearance of these two gatherings of interplanetary designs. The aftereffects of superposed investigation of the GCR power and concurrent interplanetary plasma and field boundaries [U, F, F. FV, and F U2] are plotted in Figure 2. That's what we see, like Figure 1,
the shock-related ICMEs are considerably more GCR viable than the shock-related CIRs; notwithstanding, the particular amplitudes for this situation are bigger when contrasted with those plotted in

Figure 1. The amplitudes of a large portion of the plasma/field boundaries [Qmax› F ma•x (FV)ma•x what's more, {FV)max1 are a lot bigger during the shock-related ICMEs than shock-related CIRs (see Table 1). We note that the greater part of the underlying sadness in the GCR

International Journal of Advanced Technology in Engineering and Science
Vol. No. 11, Issue No. 06, June 2023
www.ijates.com
ijates
ISSN 2348 - 7550

power happens during the initial 15 hours for shock-related ICMEs, where <F is additionally improved. This shows the significance of the violent field area in discouraging the GCR inten-sity, in concurrence with past examinations

3.2-Structures Within ICMEs and Their Influence

We next concentrate on the transient regulation because of the ICMEs related and non-related with shock. Taking into account the beginning season of these two gatherings of the ICMEs, distinguished somewhere in the range of 1995 and 2009, we play out the superposed-age examination of the vast beam power information for two neutron screens, Oulu and Newark, as well as concurrent plasma and attractive field boundaries (Figure 3). The figure shows that shock-related ICMEs are more GCR successful than those not related with shock.

These outcomes agree with the prior and references in that) underlining the impor-tance of shock/sheath district in regulating the GCR power. True to form, the abundancy of the GCR-force decline, because of the ICMEs without shock, is more modest. As respects the time profiles, there is likeness in the two cases. Be that as it may, the underlying beginning because of no-shock ICMEs is supposed to be more continuous. This noticed time conduct is presumably a measurable impact. Upgrades in different boundaries [U, F, F FV, and FV] are a lot bigger due

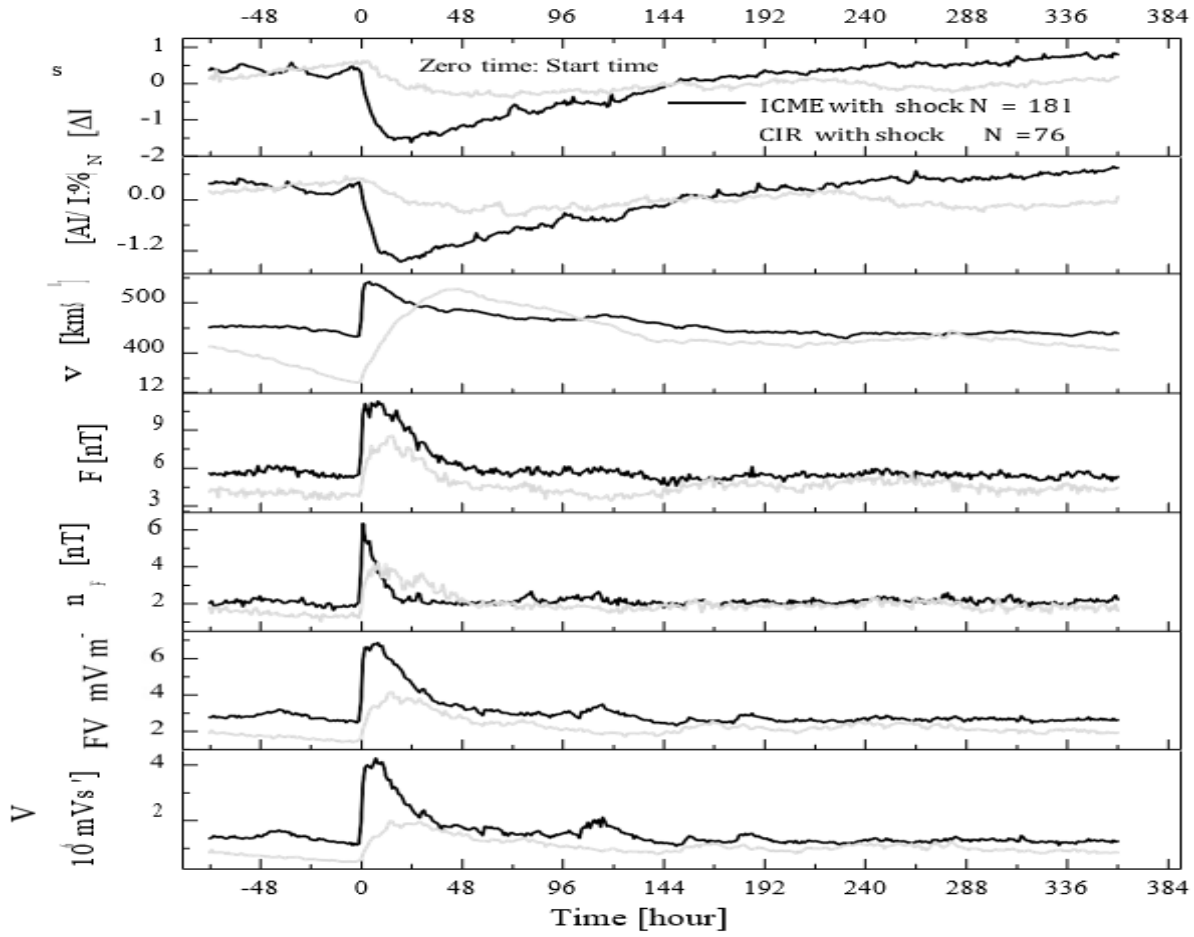

figure 2 The supcrposed-age plots of hourly information of cosmic enormous beam (GCR) power at the Oulu NM[An I/1: 9a]O , GCR power at the Newark NM [A///: %]N , plasma and attractive field boundaries [V, N, F FV, FV2] because of the ICMEs and CIRs related with (forward) shock saw during 1995 — 2009; party time (age) compares to the appearance time (hour) of the ICMEs and CIRs. N represents the quantity ofoccasions.to stun related ICMEs than those not related with shock (Table 1). These are the av-erage upsides of plasma and attractive field boundaries got from the superposed plots in Figure 3. To affirm that the distinction between ICMEs related with and without shock saw with superposed-age investigation isn't because of a few outrageous occasions, however it rather comes from the overall way of behaving of the ICMEs related/not related with shock, we have concentrated on the recurrence dispersion of these plasma and attractive field boundaries and astronomical beam decline (Forbush decline) during the section of the ICMEs related/not related with shock, by making reasonable gatherings of amplitudes of different boundaries. We additionally applied the Gaussian fit over the histograms in the initial five boards to see quantitative contrasts in mean qualities and the spread in the appropriation. For every boundary we utilize equidistant canisters of reasonable reach so all the dis- tributions comprise of a similar number of receptacles (7 to 10 containers). We utilize equidistant containers of 100 family s ' for speed, 5 nT for IMF, 1 nT for standard deviation (SD) of IMF, 2.5 mV m° l for FV, 2 mV s° 1 for FV , and 0.5 % for the GCR-power decline. These distresses-

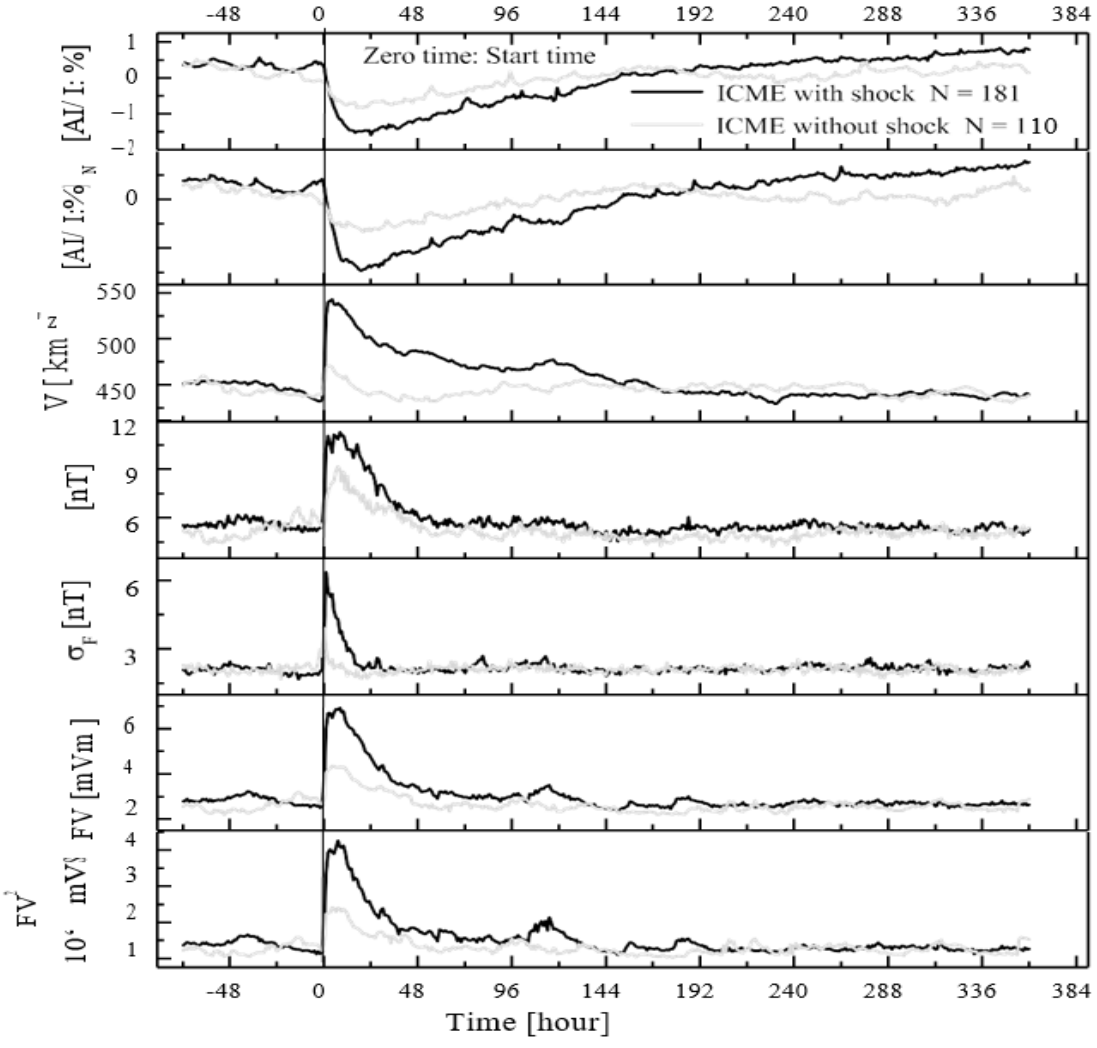

International Journal of Advanced Technology in Engineering and Science
Vol. No. 11, Issue No. 06, June 2023
www.ijates.com
ijates
ISSN 2348 - 7550

Figure 3 The superposed-epoch plots of hourly data *ot* galactic cosmic ray (GCR) intensity at the Oulu NM [A//f: 9c]
, GCR intensity at the Newark NM [A f/ *: •]N plasma and magnetic field parameters [V, *F,cr y, FV,* FV^2] due to ICMEs associated with/without shock observed during 1995 — 2009; zero hour (epoch) corresponds to the arrival time (hour) of the ICMEs. N stands for the number of events.butions for i) max ii) *F,z x,* iii) *(FV) z,,,* iv) *F* Qmax› v) *(FV*)max› and vi) GCR-intensity
decline as seen at the Newark NM are plotted in Figure 4. There is some changeability in the quantity of occasions in the various boards of Figure 4(i — v) since we barred theanomalies. In Figure 4(vi), just those ICMEs were included which delivered discouragements in the GCR force. These plots show contrasts between the dispersions o1 shock-related ICMEs and those not related with a shock, for all boundaries; the conveyance for shock-related ICMEs is moved toward higher qualities in practically this multitude of circulations. Further, the change in the pinnacles of the Gaussian-fitted bends in these plots toward higher qualities for shock-related ICMEs is additionally seen. We have applied the measurable t-trial of two examples (Figure 4(i — v)) by utilizing the Gaussian-fitted information to test the meaning of the distinction between the two conveyances.
Figure 4(vi) doesn't show a Gaussian dispersion so we apply a non-parametric (Mann Whitney) trial of two free examples. The two tests were performed utilizing a SPSS measurements programming bundle and the outcomes show that for each situation the dispersions are viewed as altogether unique at level 0.01. An importance level of 0.01 shows that there is 1 % chance of presuming that a distinction found in our review has

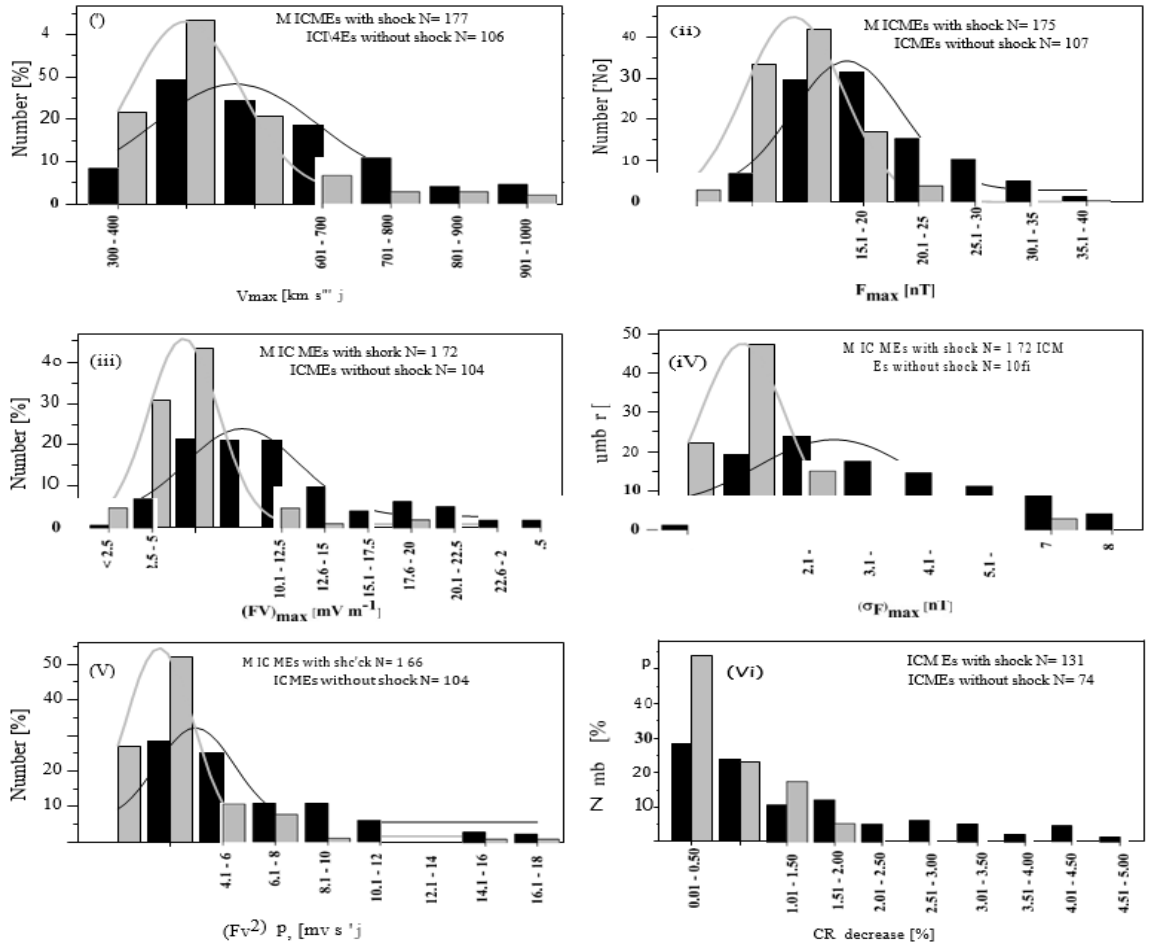

Figure 4 Regularity distribution of i) concentrated speed, [Qmax kin s*], ii) maximum IMF vector, *[Fzzz*
nT], iii) all-out electric field, *[(FV) zzz :* mV in* l], iv) maximum standard deviation in IMF vector, *[F) zz :* nT], iv) all-out *[(FV) zzz :* inV s*], and vi) CR reduction observed during the passage of ICMEs

Associated/not associated with shock Gaussian best-fit curves representing the distribution of ICMEs are also shown in the first five panels *ot* the figure. N stands for the number *ot* events considered for each histogram (see also Appendix A).happened by some coincidence. We pick a more modest worth of the importance level, for example 1 %, to be more sure of the legitimacy of the noticed outcome.The significant qualities (test sizes, implies, standard deviations, and p-values) so ob-tained are organized (see Supplement A).Having confirined the significance of shock-related ICMEs, we next consider just these ICMEs. From the ICME review/indexes we note that for a portion of the shock-related ICMEs, attractive deterrent (for example ejecta) and ICME start time is something similar while in some others ICME start time is sooner than the attractive impediment (MO) appearance time (see Jian ci o/., 2006b for subtleties as respects 'attractive hindrance' and its distinguishing proof). The for-mer class of ICMEs seems to have a forward shock simply before the MO without a sheath locale while the last classification of ICMEs has a forward shock followed by a sheath district and afterward the MO or ejecta. To concentrate on the distinctions in the GCR viability of these two gatherings of ICMEs, i.e., a) when begin time and MO time is something very similar and b) when the beginning

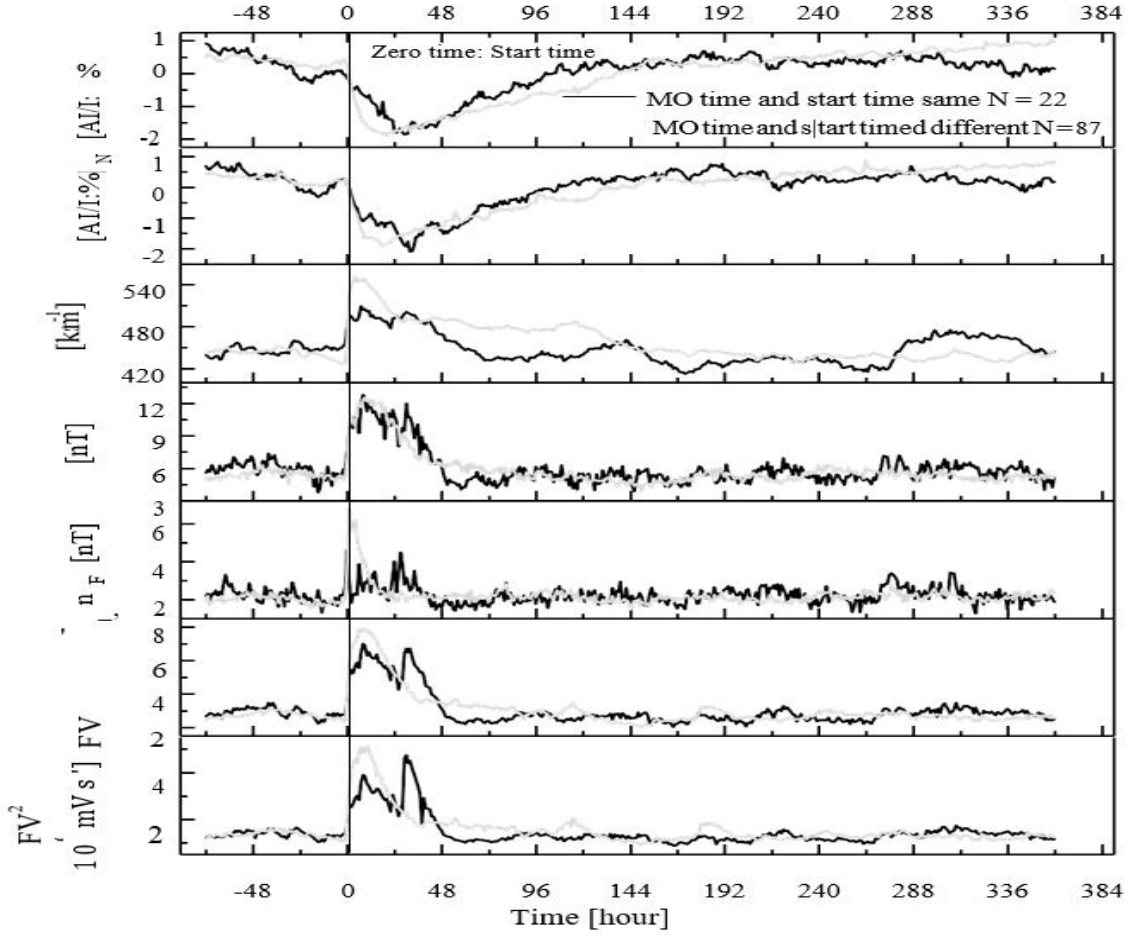

Figure S The superposed-epoch plots of hourly data of galactic cosmic ray (GCR) intensity at the Oulu NM

[k I/1: 9c] , GCR intensity at the Newark NM *[AI/1:* °]N plasma and magnetic field parameters[+. *F < V, FV]* due to ICMEs associated with shock observed during 1995 —2009; zero hour (epoch) corresponds to the time (hour) of shock arriving at same time as/different time trom magnetic obstacle (MO, ejecta). N stands for the number of events.time and MO time are unique, we have plotted the superposed-age plots concerning start season of these two gatherings of ICMEs (Figure 5). We see that on account of the two gatherings of the ICMEs the GCR-power decline begins toward the beginning time yet, on account of gathering b) ICMEs, the plentifulness is bigger (see Table 1), the underlying reduction is quicker, and the base GCR force is noticed before when contrasted with the instance of gathering a) ICMEs. In any case, a to some degree higher plentifulness at Newark when contrasted with that at Oulu because of gathering

a)-ICMEs is surprising, as the Newark cut-off inflexibility is higher. Then, we set the MO time to nothing (age) in the superposed plots of the GCR power r.v. plasma and attractive field boundaries in the two cases for example when a) the ICME start time is equivalent to that of the attractive snag, and b) when the beginning of unsettling influence and attractive obstruction time is unique. These plots are displayed in Figure 6. We see that because of the last option gathering of shock-related ICMEs despondency begins before the appearance of MO (ejecta) and two-step diminishes might be expected to such ICMEs. The second step liable to happen at the hour of MO (ejecta) and the initial step during entry of shock/sheath area (see Stick, 2000). The time profiles of F and

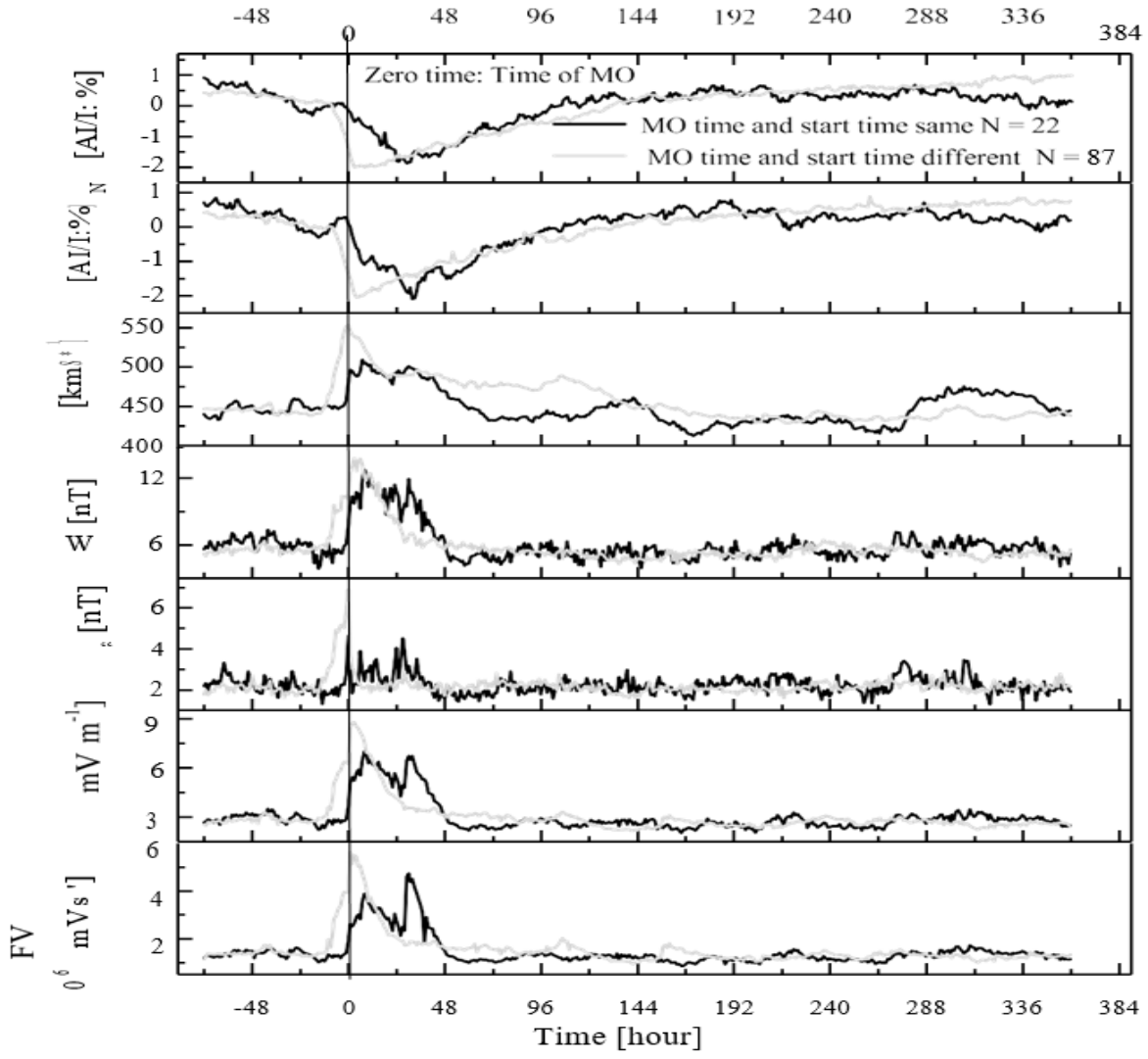

International Journal of Advanced Technology in Engineering and Science
Vol. No. 11, Issue No. 06, June 2023
www.ijates.com
ijates
ISSN 2348 - 7550

Figure 6 The superposed-epoch plots of hourly data or galactic cosmic ray (GCR) intensity at the Oulu NM [A f/ : •]o. GCR intensity at the Newark NM [A I/1: %°lN. plasma and magnetic field parameters [V, F, F FV, FV] due to ICMEs associated with shock observed during 1995 — 2009; zero hour (epoch) corresponds to the time (hour) of magnetic obstacle (MO, ejecta) arriving at same time as/different time from shocks. N Stands for the number of events.oF support this conclusion; F and off both are high during

The section of the shock/sheath district, while just a brief time after the MO time.

The following detectable element in ICMEs is the end season of the ICME, both in the ICMEs related and those not related with shock. We are intrigued to see whether GCR re-coveys begins toward the finish of the ICME structure or at some later/prior time. To concentrate on this, we have taken the end season of the ICMEs as the age (party time) for the two ICME gatherings,

a)Associated and b) not related with shock. We notice (see Figure 7) that the recuperation by and large beginnings a couple of hours before the section of the back piece of the ICMEs.It might, in any case, be noticed that separated from its value in a few areas of room research and different disciplines (see Singh and Bedridden, 2006), superposed-age examination likewise has its limits. The fine bases will be spread out except if one picks the zero age shrewdly. For instance, we can concentrate on the beginning of the shock/sheath locale by picking its tiling as the zero age, in any case, then the data as respects theejecta start is lost. On

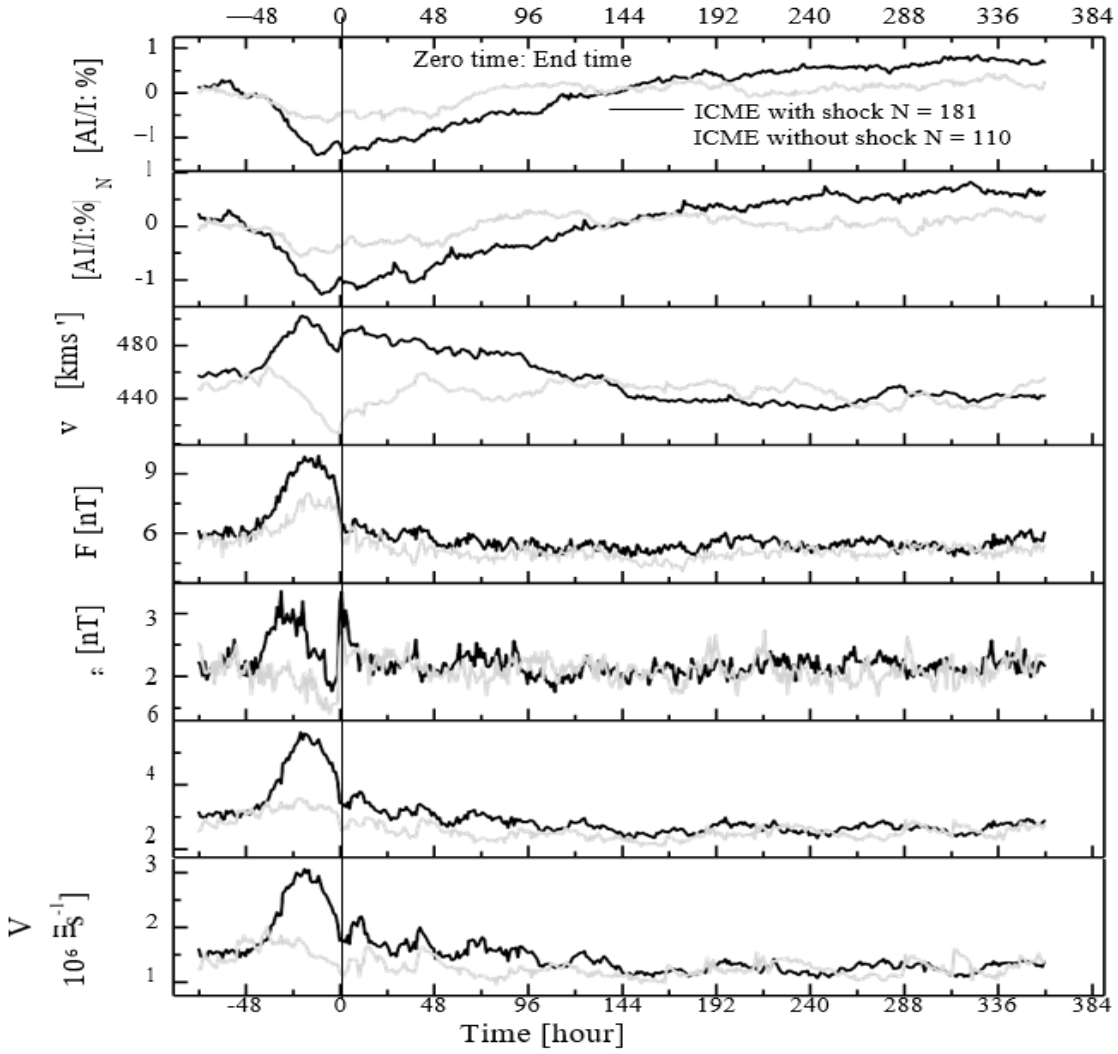

Figure 7 The superposed-epoch plots of hourly data of galactic cosmic ray (GCR) intensity at the Oulu NM [A I/1: 9a] , GCR intensity at the Newark NM [A I/I: %]N. plasma/and magnetic field parameters [V, F, o F , FV, FV2] due to ICMEs associated with/without shock observed during 1995 — 2009; zero hour (epoch) corresponds to the end time (hour) of the ICMEs. N stands for the number of events.the other hand, in the event that we pick the ejecta start as the zero age, we can take a gander at the ejecta foundation independently.

3.3. Structures Within CIRs and Their Influence

We have concentrated on the impacts of two gatherings of CIRs for example a) CIRs with a forward shock, and a)CIRs without forward shock. We performed superposed-age examination of the GCR in-strained quality ve. plasma and attractive tield boundaries [V, +. F + V, and NV*] concerning the beginning season of these two gatherings of CIRs (Figure 8). We track down a huge distinction in amplitude of sorrow in the GCR force (Table 1) because of CIRs with shock and CIRs without shock; the previous gathering of CIRs being more GCR successful than the last option bunch albeit the recuperation time profiles in the two cases are practically comparable. Upgrades in the normal plasma and attractive field boundaries are fairly bigger (Table 1) and seriously fluctuating on account of CIRs with forward shock (see Figure 8).

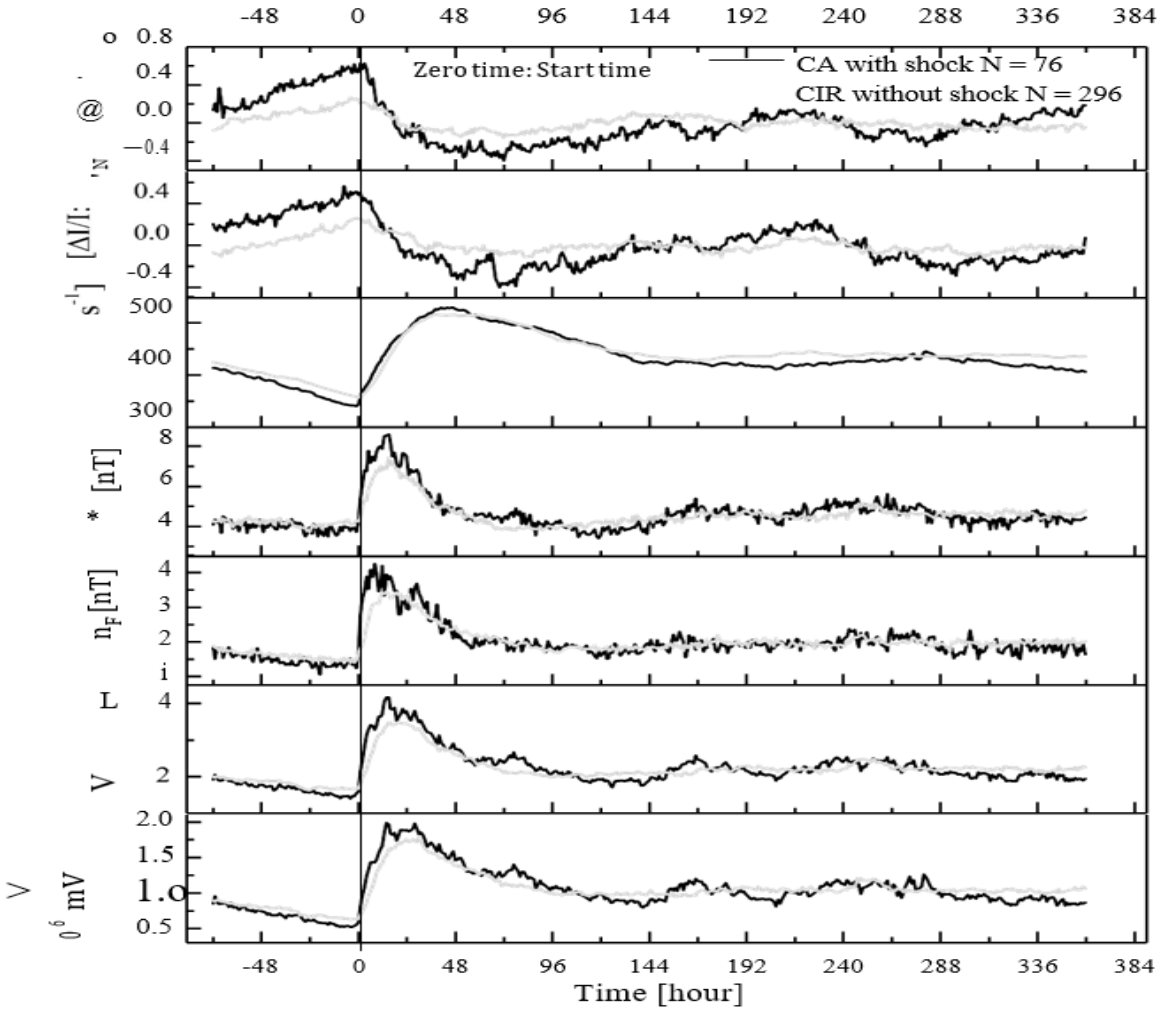

International Journal of Advanced Technology in Engineering and Science
Vol. No. 11, Issue No. 06, June 2023
www.ijates.com
ijates
ISSN 2348 - 7550

Figure 8 The superposed-epoch plots of hourly data of galactic cosmic ray (GCR) intensity at the Oulu NM *[k I/ I:* 9a]$_O$, GCR intensity at the Newark NM *[k I/1:* 9a]$_N$, plasma and magnetic field parameters [V, *F, F > V, FV]* due to ICMEs associated with/without shock observed during 1995 — 2009; zero hour (epoch) corresponds to the arrival time (hour) of CIRs associated with/without shock. N stands for the number ot events.

What's more, we likewise concentrated on the circulation of boundaries [max Floy, (F)max F)mnx • also (F V2)ina.] and the GCR-power decline, as seen at GCR Newark NM, during the section of these two sorts of CIRs (Figure 9). There is likewise a little fluctuation in the number of occasions in the various boards of Figure 9(i — v) because of prohibition of the anomalies, comparatively to Figure 4. In Figure 9(vi) just those CIRs were taken which delivered dejections in the GCR power. To test the meaning of the distinction between the two conveyances, we again applied the factual t-trial of two examples for Figure 9(i — v) by utilizing Gaussian-fitted information and non-parametric (Mann Whitney) trial of two free examples for Figure 9(vi). The tests were performed utilizing a SPSS measurements programming bundle. We found the p-an incentive for m hatchet (0•754), for (FV),z z (0.0266), and for (F V2)max (0•930) and consequently the two methods for these dispersions are not essentially unique. The distinction of the circulation implies between CIRs with and without shock for Qmax, F)>,, , and GCR decline is viewed as genuinely huge at the importance level 0.01.The significant boundaries of the examination are displayed in AddendumB.

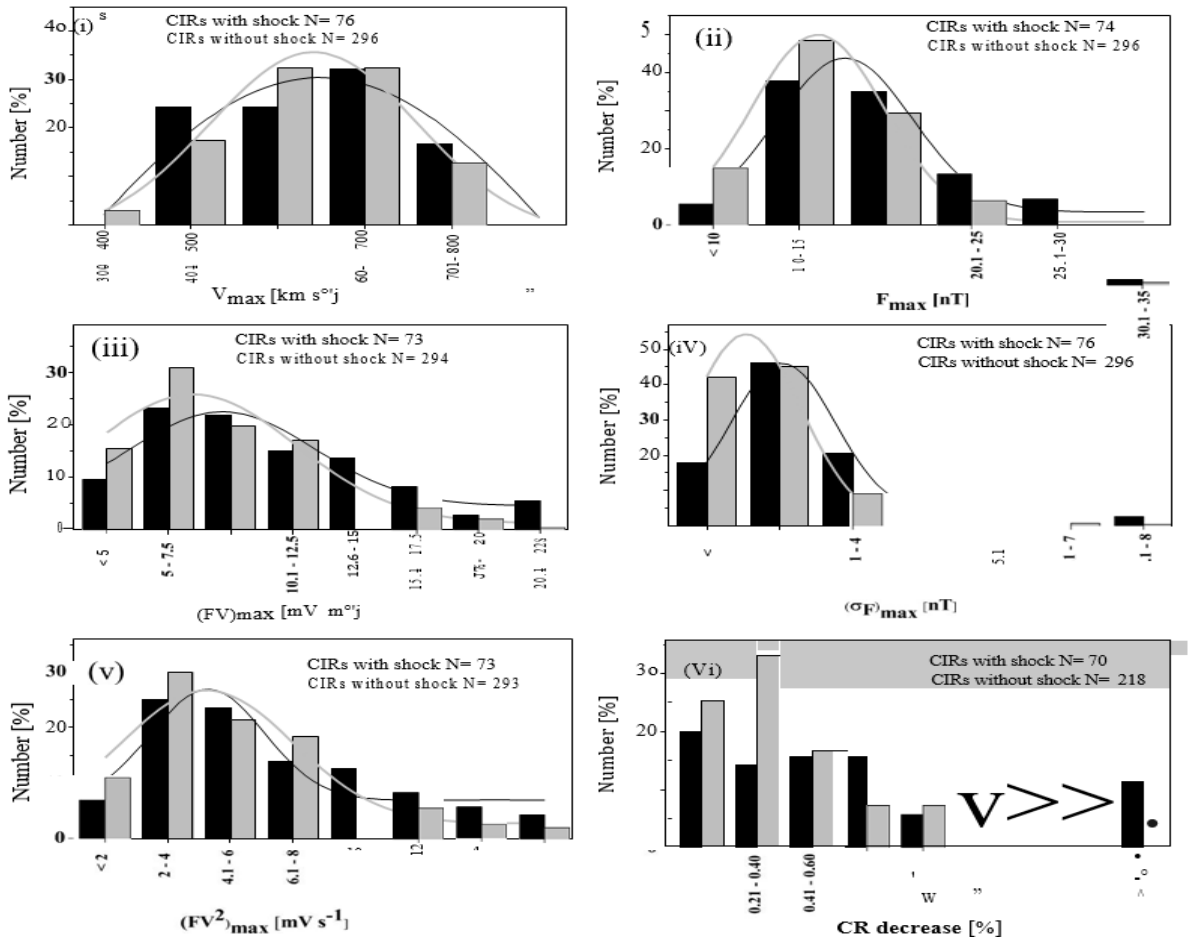

Figure 9 Frequency distribution of i) maximum speed, [Vp : km s], ii) maximum IMF vector, [Qmax nT], iii) maximum electric field, *[(FV)PSs:* mV m*^{1}], iv) maximum standard deviation in IMF vector, *[F) zz:* nT], iv) maximum *[(FV^{2})may:* tip S* ^{1}], and vi) CR decrease observed during the passage ofCIRs associated with forward shock/not associated with shock. Gaussian best-fit curves representing the dis- tribution of CIRs are also shown in the first five panels of the figure. N stands for the number of eventsconsidered for each histogram A stream interface (SI) can be distinguished inside CIRs. At the SI, attractive field fluctua-tions are supposed to be high. Hence, it will be fascinating to look for the job of SI in impacting the GCR-power time profile. For this reason, we originally separated the CIRs into two gatherings, I) CIRs with shock and ii) CIRs without shock, and afterward we applied the strategy for the superposed-age examination to grandiose beam ve. plasma and attractive field information with ref-erence to the SI time, independently for the two gatherings of CIRs.

We note that the downturn in the GCR power begins sooner than zero time, and it arrives at the base worth modify the SI appearance. The upgrades in interplanetary boundaries as of now are likewise noticeable in the superposed plots (Figure 10). It shows that the SI adds to the adjustment of cosmic inestimable beams during the section of CIRs, albeit the downturn begins prior at the appearance of CIRs.

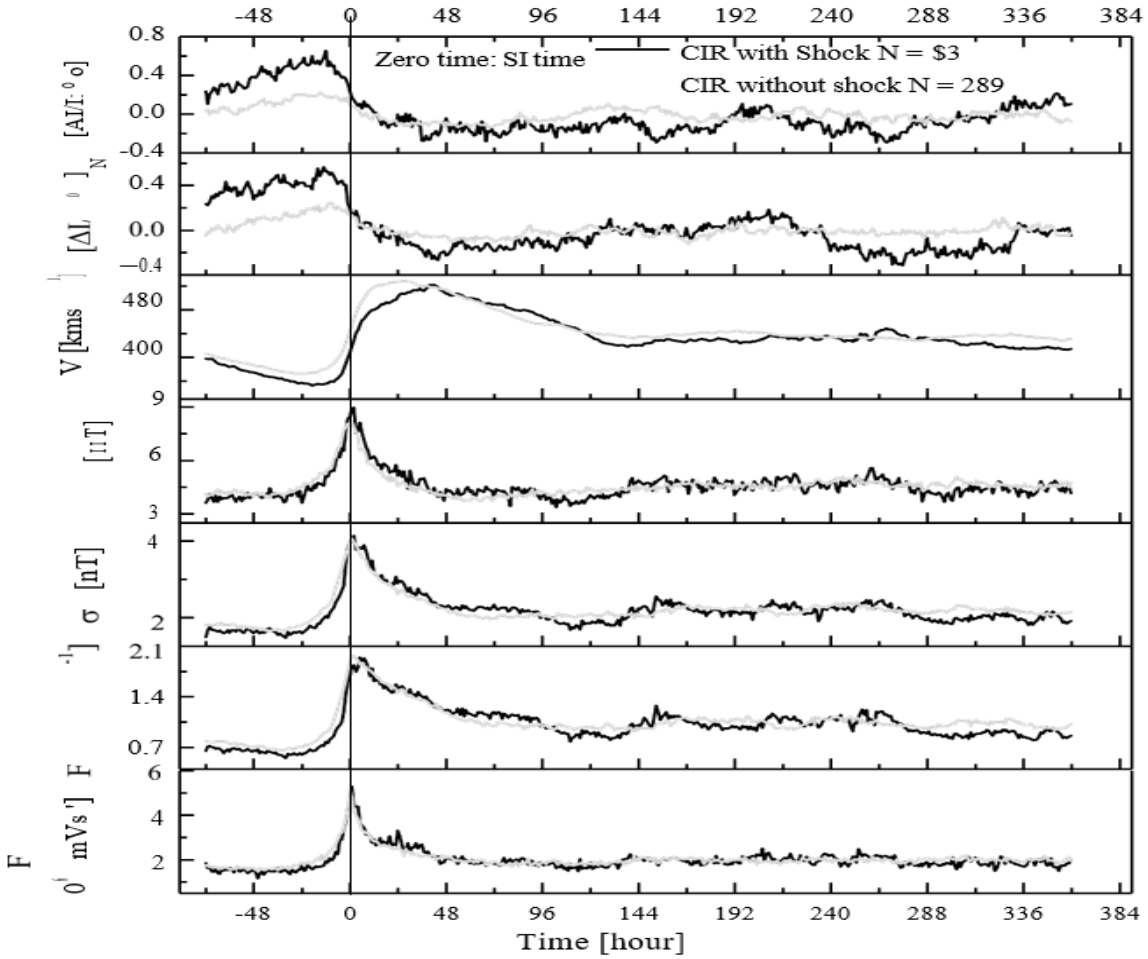

Figure 10 The superposed-epoch plots ot hourly data or galactic cosmic ray (GCR) intensity at the Oulu NM [A f/: %], GCR intensity at the Newark NM [A I/1: °lN. plasma and magnetic field parameters [V, F, F FV, FV2] due to CIRs associated with/without shock observed during 1995 — 2009; zero hour (epoch) corresponds to the stream interface (SI) time (hour) of the CIRs. N stands for the number of events.

To check whether the downturn in the GCR power that typically begins at the appearance of CIR per-sits after its section for quite a while or begins recuperating, we have considered two gatherings of CIRs for example CIRs with forward shock and CIRs without forward shock. Then the superposed-age investigation is finished by orchestrating the information as for the end season of two gatherings of CIRs independently (see Figure 11). We see that in the two cases, the GCR recuperation begins a couple of hours after section of CIRs, albeit gradually, particularly on account of CIRs with forward shock.From the superposed-age plots of different boundaries displayed in a portion of the figures (Figures 1, 2, 3, and 8), we have decided the spans of the principal stages and recovery stages (Table 2). From these found the middle value of plots, the term of the principal stages (begin to least) due to a) shock-related ICMEs (then it IS hours), b) ICMEs without shock (20 hours), c) CIRs with shock (52 hours), d) CIRs without shock (56 hours). The cor-answering term of the recuperation stage is 172 hour (7 days) for ICME with shock and 95 hours (4 days) for ICMEs without shock. Be that as it may, on account of CIRs, both with and without shock, the specific span of the recuperation stage not set in stone

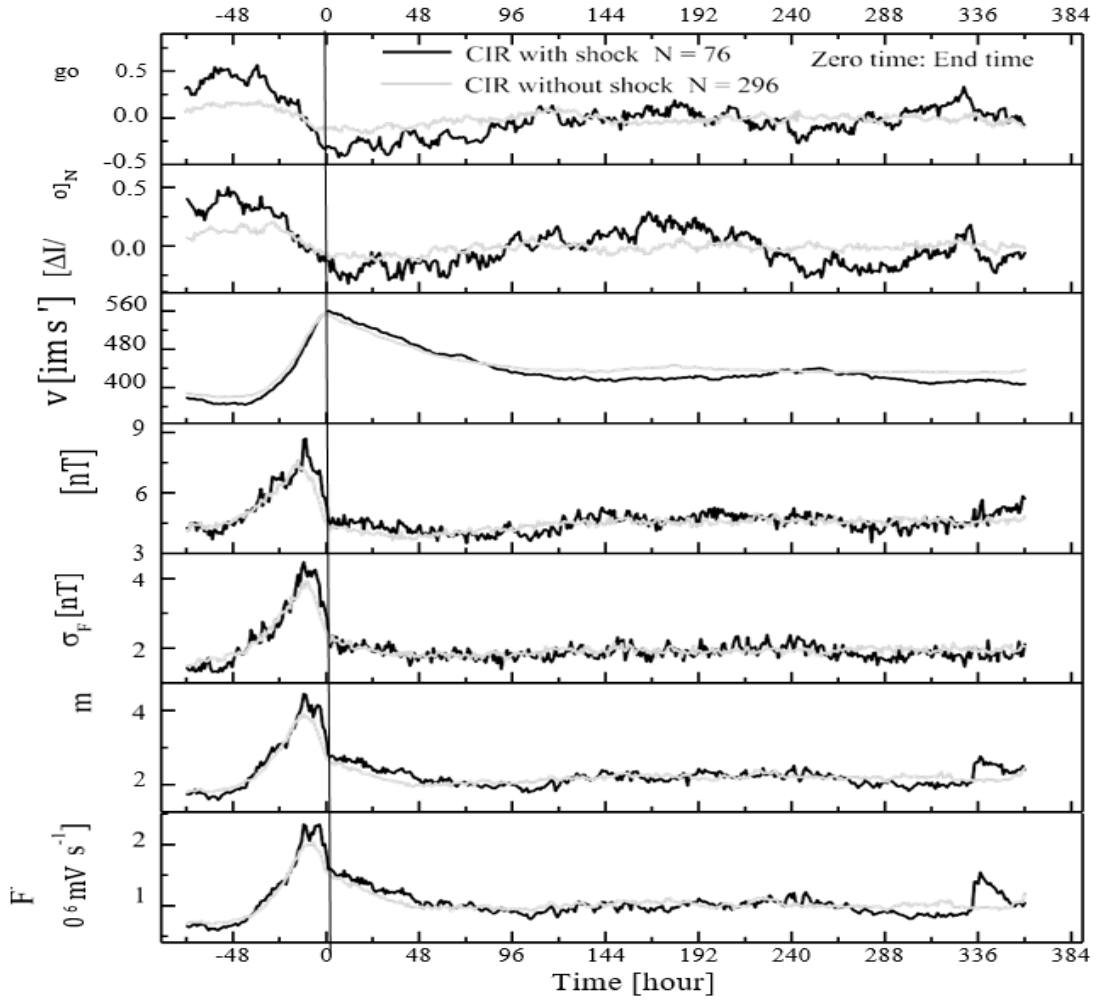

Figure 11- The superposed-epoch plots of hourly data of galactic cosmic ray (GCR) intensity at the Oulu NM *[A I/I:* 9c] $_{O}$, GCR intensity at the Newark NM *[AI/I:* %]$_{N}$, plasma and magnetic field

parameters [V,*F, F FV,* FV^2] due to CIRs associated with/without shock observed during 1995—2009; zero hour (epoch) corresponds to the end time (hour) of the CIRs. N stands *too* the number of events. since the force doesn't recuperate to its pre-decline level inside the picked time between val. Albeit the fundamental stage spans of individual Forbush diminishes (FDs) may change, the typical primary stage length of FDs was assessed to be 13 4.5 hours A superposed-age investigation of the infinite beam information concerning attractive mists has demonstrated the primary stage length to be 21 — 24 hours The consequences of our superposed-age examination with respect to the fundamental stage terms for example 18 hours for shock-related ICMEs and 20 hours for no-shock ICMEs are in reasonable concurrence with these prior discoveries. The recuperation of FDs may likewise differ (3 to 10 days) with a typical time of 5 days. The consequences of our review in view of the superposed-age examination supplement these discoveries. They further demonstrate that the recuperation term might be, as a rule, more limited because of the ICMEs not
related with shock and bigger because of shock-related ICMEs. The discouragements because of CIRs are, as a rule, de-valor increasingly slow for a more extended time frame than those because of ICMEs. The greater part of the prior investigations are restricted to the investigation of individual/normal miseries because of CIRs/fast streams furthermore, got many intriguing outcomes about their time history, their relationship with plasma and attractive field boundaries (c.g. see Richardson, 2004, and references in that). Be that as it may, we concentrate on these viewpoints by isolating them into two gatherings for example those related and not related with shock, and we concentrated on the distinctions in their effects.

Notwithstanding contrasts in terms and time profiles of the primary stage because of ICMEs and CIRs, we notice, based on midpoints, that the GCR-power melancholy because of the ICMEs with shock is 2.3 times higher than that because of the ICMEs without shock. Simi-larly CIRs with shock delivered 2.4 times more sorrow in the GCR power than CIRs without shock. At the point when we look at shock impacts in ICMEs and CIRs, we see that ICMEs with shock are two times as GCR compelling when contrasted with shock-related CIRs. A similar ratio approximately holds for no-shock ICMEs and CIRs. Accordingly apparently the shock/sheath impact isn't comparatively GCR powerful for both ICMEs and CIRs. Richardson and Stick (2011) contrasted the shock impact with the complete melancholy in the GCR power. That's what they saw, despite the fact that there are huge occasion to-occasion varieties in the shock and ICME commitments to the complete melancholy, in any case, on the normal the size of shock impact in ICMEs is 55 do of the all out change. It infers that the shock and the ICME impacts are practically equivalent on assert age. Our outcomes agree with these outcomes, which show that the shock-related ICMEs are about two times as GCR ełfective when contrasted with the ICMEs without shock. From these found the middle value of (superposed age) plots, we have attempted to find the plasma and attractive held boundaries whose time variety best corresponds with the time variety of the GCR force, independently during fundamental and recuperation stages because of the ICMEs and CIRs. Table 2 shows the worth of single Pearson's relationship coefficient's [fin alongside the comparing p-values. We find that out of the boundaries considered, the time variety of the IMF vector [F] best relates with the GCR power during the primary stage, while it is the time variety ołthe speed [V] that best connects with the time variety of the GCR force during recuperation, because of the ICMEs with shock as well as ICMEs without shock. Nonetheless, it is the time variety of the speed [V] that best connects with the time variety of the GCR power both during the fundamental as well as recuperation stages because of CIRs with and without shock (see Table 2).Sadness in the GCR force during Forbush diminishes being associated with mag- noetic field strength have likewise been accounted for before revealed a decent relationship be tween's FD ampli-tude and most extreme attractive field in attractive mists presumed that the meld strength B firmly impacts the have observed that the downturn in the GCR force is connected with the sufficiency of the interplan-etary field vector during section of the ICMEs with deferent highlights. The tweak on the vast beam force in CIRs related with high velocity sun oriented breeze streams connected with the sun based breeze speed increment have been accounted for detailed that these discouragements follow the progressions in the sun oriented breeze speed. Richardson, Wibberenz, and Stick (1996) additionally observed that high velocity streams are accoinpanied by miseries in the GCR force and will quite often be against corresponded with the sun oriented breeze speed Albeit these examinations had

the option to explain numerous parts of the regulation because of CIRs and fast streams, the current work studies the elfects of CIRs with a bigger information base by isolating them in two gatherings ice. those related and non-related with forward shock. We play likewise concentrated on the part of various highlights of CIRs, for example forward shocks and stream collaboration locales on the sufficiency and time profile ox GCR-power misery

Summary and Conclusions

In light of our examination of the enormous beam power along with interplanetary plasma and field boundaries during the entry of the ICMEs and CIRs during Sunlight based Cycle 23 (1995 — 2009), a synopsis of our decisions is given underneath.

- In concurrence with prior discoveries, ICMEs are viewed as more successful in balancing the GCR power when contrasted with CIRs, despite the fact that the improvement in sunlight based breeze speed because of CIRs is bigger than the upgrade because of the ICMEs. Be that as it may, the typical amplitudes ot interplanetary attractive and electric field vectors are bigger during the section of the ICMEs. Notwithstanding amplitudes, the time profiles of GCR-force dejections are additionally unique because of these two interplanetary designs, in concurrence with prior discoveries.
- The typical plentifulness of GCR-power gloom for ICMEs is 1.5 % when contrasted with that for CIRs, which is 0.5 9c. The proportion of GCR sorrows for ICMEs with shock to ICMEs without shock is around 2.3, and the proportion of power sadness because of shock-related CIRs to non-shock CIRs is about the very, or at least, 2.4.
- The GCR-power melancholy overall beginnings at the appearance of the ICMEs, regardless of whether related with shock; nonetheless, the downturn is a lot bigger because of shock-related ICMEs, in concurrence with past examinations, again stressing the significance of shock/sheath district in transient balance of GCRs.
- The GCR recuperation, attar an underlying period of power decline, begins before the entry of the back piece of the ICME.
- The CIRs with a forward shock are more viable in discouraging the GCR power than those not related with a shock, albeit the time profiles of the GCR force in the two cases are practically comparable; a sluggish sorrow to a base, and a long and slow recuperation.
- At the appearance of stream interface inside CIRs, a further diminishing in the GCR power by and large occur.
- From the typical plots got from superposed-age examination, the time variety of the GCR power because of ICMEs, during the principal (decline) stage, is viewed as better connected with the time variety of the attractive field vector. Nonetheless, the time variety of sun based breeze speed better connects with the GCR power during this stage, on account of a diminishing because of CIRs. During the recuperation stage, the worldly variety of the GCR force is viewed as better connected with synchronous varieties in the sunlight based breeze speed, during the recuperation of reduction both because of ICMEs as well as CIRs. These outcomes offer further help to prior results that detailed great relationship between's the plentifulness of the GCR power decline and interplanetary attractive field strength during Forbush diminishes. Further, it additionally agrees with the decline in power related with the expansion in sun based breeze speed during corotating discouragement in the GCR force.
- The downturn is viewed as biggest for I) shock-related ICMEs and, besides, ii) for shock-related ICMEs where the ejecta are gone before by a shock/sheath district (ICMEs with MO start unique). This not just shows the job of a violent shock/sheath district, yet additionally it demonstrates the job of ejecta.

ijates
ISSN 2348 - 7550

Table 3 The calculated mean, normal deviation (SD) for each delivery, and t-values and p-values forevery one pair of distribution (ICMEs associated with/without shock) using statistical t-test of two independentsamples at significance level 0.01 with the help of Gaussian-fitted parameters for plasma and magnetic field parameters [Vp • max *(FV)jjjj* : ℓ)jjy $(F^{J\,2})_{max}$]

Parameters	Structures	Mean	SD	t-value	p-value
max	ICMEs with shock N_i = 177	522.58	120.17	5.61	4.83 x 10*'
	ICMEs without shock N_2 106	449.07	80.71		
F_{max}	ICMEs with shock N_i = 175	16.02	4.90	8.24	6.62 x 10^{*15}
	ICMEs without shock N_2 107	11.24	4.41		
(FV)zp	ICMEs with shock N_i = 172	8.97	3.27	9.69	2.71 io ^{19}
	ICMEs without shock N_2 104	5.58	2.02		
(F)max	ICMEs with shock N_i = 172	2.89	1.25	11.53	2.06 x 10^{*2}
	ICMEs without shock N_2 108	1.39	0.69		
$(F^{J\,2})$	ICMEs with shock N_1 = 166	3.95	1.49	7.74	2.02 x $10^{*\,1n}$
	ICMEs without shock N_2 104	2.58	1.30		

International Journal of Advanced Technology in Engineering and Science
Vol. No. 11, Issue No. 06, June 2023
www.ijates.com
ijates
ISSN 2348 - 7550

Table 4 The intended mean, normal deviation (SD) for each delivery, t-values and p-values for eachpair of distribution (ICMEs associated with/without shock) using arithmetical tests (two sample t-test using raw data of , **Flax** $(FV)_{max}$, (N)max (FV^2) ; non-parametric (Mann Whitney) test of two indecent- dent samples using raw data of GCR-intensity decrease) at significance level 0.01 with the help of an SPSS statistics software package.

Parameters	Structures	Mean	SD	t-value	p-value
V_{max}	ICMEs with shock N_i = 177	573.73	151.14	4.65	< 0.01
	ICMEs without shock N_2 106	491.51	130.83		
F_{max}	ICMEs with shock N_i = 175	18.13	6.67	8.22	< 0.01
	ICMEs without shock N_2 107	11.99	5.00		
$(FV)_{max}$	ICMEs with shock N_i = 172	11.00	5.32	8.55	< 0.01
	ICMEs without shock N_2 104	6.13	2.96		
	ICMEs with shock N_i = 172	3.63	1.77	8.87	< 0.01
$(\sigma_F$	ICMEs without shock N_2 108	1.88	1.32		
$(FV^2)_{max}$	ICMEs with shock N_1 166	6.23	3.94	6.79	**<0.01**
	ICMEs without shock N_2 104	3.29	2.51		
CR decrease	ICMEs with shock N_1 = 131	0.72	0.54	-	< 0.01
	ICMEs without shock N_2 = 74	0.47	0.38		

Table S The calculated mean, standard deviation (SD) *Nov* each distribution, and t-values, p-values for each pair of distribution (CIRs associated with/without shock) using the statistical t-test of two independent Sam- plus at significance level 0.01 with the help of Gaussian-fitted parameters for plasma and magnetic field parameters [max Qmax › *(FV)* max› *F)* max *(FV'* may-

Parameters	Structures	Mean	SD	t-value	p-value
V_{max}	CIRs with shock N_i = 76	59b.50	326.52	0.31	0.754
	CIRs without shock N3 = 296	591.18	119.79		
F_{max}	CIRs with shock N_1 = 74	15.14	5.91	3.18	0.0016
	CIRs without shock N2 = 296	13.55	3.67		
( )inax	CIRs with shock N_1 73	5.41	3.70	2.23	0.0266
	CIRs without shock N2 = 294	7.23	4.14		
$(\sigma_F)_{max}$	CIRs with shock N_i = 76	2.55	0.71	5.61	3.96 x 10
	CIRs without shock N2 = 296	2.01	0.76		
(FV') zzz	CIRs with shock N_i = 72	4.28	1.79	0.088	0.930
	CIRs without shock N2 = 293	4.25	2.73		

Table 6 The calculated mean, standard deviation (SD) lor each distribution, t-values and p-valucs for each pair of distribution (CIRs associated with/without shock) using statistical tests (two sample t-test using raw data 0F Qmax Qmax› *(FV)* ng_X• ^F)inax (^{2})inax i non-parametric (Mann Whitney) test of two independent samples for raw data of GCR-intensity decrease) at significance level 0.01 with the help of an SPSS statistics software package. The p-values are given up to the third decimal place only.

Parameters	Structures	Mean	SD	t-value	p-value
V_{max}	CIRs with shock Nt = 76	596.05	108.86	0.527	0.598
	CIRs without shock N2 296	586.55	105.50		
Q jjjax	CIRs with shock Nt = 74	16.62	5.26	4.52	< 0.01
	CIRs without shock N_2 = 296	14.00	4.24		
$(FV)_{max}$	CIRs with shock N 73	10.?3	4.69	3.16	0.002
	CIRs without shock N_2 = 294	5.65	3.79		
(f)max	CIRs with shock Nj 76	2.96	1.28	5.51	< 0.01
	CIRs without shock N2 = 296	2.26	0.69		
$(F^{2})_{max}$	CIRs with shock Nt = 72	6.36	3.70	2.13	0.034
	CIRs without shock N2 293	5.42	3.25		
CR decrease	CIRS with shock Nt = 70	1.41	1.23	-	<0.01
	CIRs without shock N_2 = 218	0.59	0.45		

References

1. Sbardeen 2002, Ap&SS, 281, 651
2. Sbardeen,Yadav, R. S., & Yadav, N. R. 1986, Sol. Phys., 105, 413
3. Kabila, J. J., Catalan, E., Hidalgo, M. A., Medina, J., & Rodiguez-Pacheco, J. 2013, Sol. Phys., DOI:
4. Bothmer, V., & Schwenn, R. 1998, Ann. Geophys., 16, 1
5. Alzhra, A., Lara, A., Echer, E., et al. 2009, A&A, 498, 885
6. Burlaga, L. F., Sittler, E., Mariani, F., & Schwenn, R. 1981, J. Geophys. Res., 86, 6673 Candia, J., & Roulet, E. 2004, J. Cosmol. Astropart. Phys., 10, 7
7. Cane, H. V. 2000, Space Sci. Rev., 93, 55
8. Cane, H. V., Richardson, I. G., & Wibberenz, G. 1995, Proc. 24th Int. Cosmic Ray Conf., 4, 377 [
9. Casse, F., Lemoine, M., & Pelletier, G. 2002, Phys. Rev. D, 65, 023002
10. de Simone, N., di Felice, V., Gieseler, J., et al. 2011, ASTRA, 7, 425]
11. Effenberger, F., Fichtner, H., Scherer, K., et al. 2012, ApJ, 750, 108
12. Giacalone, J., & Jokipii, J. R. 1999, ApJ, 520, 204
13. Hayashi, Y., Aikawa, Y., Gopalakrishnan, N. V., et al. 2005, Nucl. Instrum. Meth. A, 545, 643
14. Heber, B., Gieseler, J., Dunzlaff, P., et al. 2008, ApJ, 689, 1443

15. Huttunen, K. E. J., Schwenn, R., Bothmer, V., & Koskinen, H. E. J. 2005, Ann. Geophys., 23, 625
16. Kubo, Y., & Shimazu, H. 2010, ApJ, 720, 853
17. Kuwabara, T., Bieber, J. W., Evensen, P., et al. 2009, J. Geophys. Res., 114, 05109
18. Lara, A., Flandes, A., Alzhra, A., & Subramanian, P. 2011, J. Geophys. Res., 116, CiteID A12102
19. Leblanc, Y., Dulk, G. A., Bougeret, J.-L., et al. 1998, Sol. Phys., 183, 165
20. Lockwood, J. A., Webber, W. R., & Debrunner, H. 1991, J. Geophys. Res., 96, 11587
21. Lynch, B. J., Zurbuchen, T. H., Fisk, L. A., & Antiochos, S. K. 2003, J. Geophys. Res., 108, 1239
22. Manoharan, P. K., Kojima, M., Gopalswamy, N., et al. 2000, ApJ, 530,
23. Matthaeus, W. S., Qin, G., Bieber, J. W., & Zank, G. P. 2003, ApJ, 590, L53
24. Nonaka, T., Hayashi, Y., Ito, N., et al. 2006, Phys. Rev. D, 74, 052003 25. Oh, S. Y., & Yi, Y. 2012, Sol. Phys., 280, 197
26. Poomvises, W.,Zhang, J.,Olmedo, O., 2010, ApJ, 717, L159
27. Reames, D. V., Kahler, S. W., & Tylka, A. J. 2009, ApJ, 700, 196
28. Richardson, I. G., &Cane, H. V. 2011, Sol. Phys., 270, 609
29. Sanderson, T. R., Beeck, J., Marsden, G. R., et al. 1990, Proc. 21st Int. Cosmic Ray Conf., 6, 251
30. Shalchi, A. 2010, ApJ, 720, L127
31. Schwenn, R., Dal Lago, A., Huttunen, E., & Gonzalez, W. D. 2005, Ann. Geophys., 23, 1033 32. Spangler, S. R. 2002, ApJ, 576, 997
33. Subramanian, P., & Vourlidas, A. 2007, A&A, 467, 685
34. Subramanian, P., Antia, H. M., Dugad, S. R., et al. 2009, A&A, 494, 1107
35. Tautz, R. C., & Shalchi, A. 2011, ApJ, 735, 92
36. Vourlidas, A., Lynch, B. J., Howard, R. A., & Li, Y. 2012, Sol. Phys., 192V: DOI:
37. Wang, Y., Zhou, G., Ye, P., Wang, S., & Wang, J. 2006, ApJ, 651,
38. Wibberenz, G., le Roux, J. A., Potgieter, M. S., & Bieber, J. W. 1998, Space Sci. Rev., 83, 309
39. Yu, X. X.,Lu, H.,Le, G. M., &Shi, F., 2010, Sol. Phys., 263, 223
40. Zhang, G., & Burlaga, L. F. 1988, J. Geophys. Res., 93, 2511